Supporting Information

Designing Asymmetrical Isomer to Promote LUMO Energy Level and Molecule Packing of Non-fullerene Acceptor for Polymer Solar Cells with 12.6% Efficiency†

Wei Gao,‡[ab] Qiaoshi An,‡[c] Cheng Zhong,[a] Zhenghui Luo,[a] Ruijie Ming,[a] Miao Zhang,[c] Yang Zou,[b] Feng Liu,*[d] Fujun Zhang*[c] and Chuluo Yang*[ab]

[a] Department of Chemistry, Hubei Key Lab on Organic and Polymeric Optoelectronic Materials, Wuhan University, Wuhan, 430072, People's Republic of China
E-mail: clyang@whu.edu.cn
[b] College of Materials Science and Engineering, Shenzhen University, Shenzhen, 518060, People's Republic of China
[c] Key Laboratory of Luminescence and Optical Information, Ministry of Education, Beijing Jiaotong University, Beijing, 100044, People's Republic of China
E-mail: fjzhang@bjtu.edu.cn
[d] Department of Physics and Astronomy, and Collaborative Innovation Center of IFSA (CICIFSA), Shanghai Jiaotong University, Shanghai 200240, P. R. China
E-mail: fengliu82@sjtu.edu.cn
† The two authors contribute equally

Synthesis

Diethyl 2,5-dibromoterephthalate (compound **1**), thiopnene, dithieno[3,2-*b*:2',3'-*d*]thiophene, 1-bromo-4-hexylbenzene, Bis(triphenylphosphine)palladium(II) dichloride ($Pd(PPh_3)_2Cl_2$) and polymer donor of PBDB-T were purchased from commercial sources. All solvents were used without further purification unless otherwise stated. Tetrahydrofuran (THF) was further dried by using potassium sodium alloy under refluxing condition. The end group (EG) of 2-(1-methyl-6-oxo-5,6-dihydro-4H-cyclopenta[c]thiophen-4-ylidene)malononitrile (CPTCN-M) and MeIC were synthesized according to our previous work.

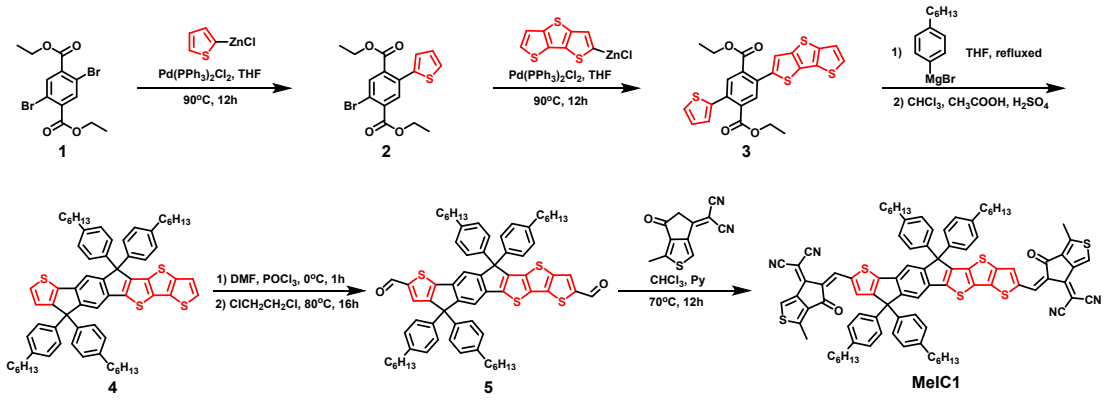

Scheme S1 The synthetic route of MeIC1.

Synthesis of ***diethyl 2-bromo-5-(thiophen-2-yl)terephthalate (compound 2)***: To a stirring solution of thiophene (500 mg, 5.95 mmol) in dry THF was dropwise added *n*-BuLi (2.38 M, 2.5 ml) at 0°C under argon atmosphere. After keeping stirring at 0°C for one hour, an anhydrous zinc chloride solution in THF (1 M, 6 ml) was dropwise added within 10 min, and the solution was allowed to stir at 0°C for another one hour. Then, compound **1** (2.26 g, 5.95 mmol) and $Pd(PPh_3)_2Cl_2$ (209 mg, 0.30 mmol) were added to the solution and refluxed with a refluxing device under argon protection for 12 hours. After cooling to room temperature, water was added and extracted with dichloromethane. The collected organic phase was dried with anhydrous Na_2SO_4 and then concentrated. The residue was purified by silicon chromatography using petroleum ether/ ethyl acetate (12:1 v/v) as eluent to give the product as an pale yellow oil (1.37 g, 60%). ^{1}H NMR (400 MHz, $CDCl_3$), δ (ppm): 7.99 (s, 1H), 7.85 (s, 1H), 7.40 (dd, J_1 = 1.6 Hz, J_2 = 2.0 Hz, 1H), 7.06-7.08 (m, 2H), 4.43 (q, J = 7.2 Hz, 2H), 4.22 (q, J = 7.2 Hz, 2H), 1.41 (t, J = 7.2 Hz, 3H), 1.16 (t, J = 7.2 Hz, 3H); ^{13}C NMR (100 MHz, $CDCl_3$), δ (ppm): 166.58, 165.29, 139.79, 135.30, 134.93, 134.48,

133.49, 133.29, 127.42, 127.13, 126.69, 120.61, 62.16, 61.91, 14.21, 13.81; MS *m/z*: [M] calcd. for $C_{16}H_{15}BrO_4S$, 381.99; found, 382.00.

Synthesis of ***diethyl 2-(dithieno[3,2-b:2',3'-d]thiophen-2-yl)-5-(thiophen-2-yl)terephthalate (compound 3):*** To a stirring solution of dithieno[3,2-*b*:2',3'-*d*]thiophene (666 mg, 3.39 mmol) in dry THF was dropwise added *n*-BuLi (2.38 M, 1.43 ml) at 0°C under argon atmosphere. After keeping stirring at 0°C for one hour, an anhydrous zinc chloride solution in THF (1 M, 3.4 ml) was dropwise added within 10 min, and the solution was allowed to stir at 0°C for another one hour. Then, compound **3** (1.3 g, 3.39 mmol) and $Pd(PPh_3)_2Cl_2$ (119 mg, 0.17 mmol) were added to the solution and refluxed with a refluxing device under argon protection for 12 hours. After cooling to room temperature, water was added and extracted with dichloromethane. The collected organic phase was dried with anhydrous Na_2SO_4 and then concentrated. The residue was purified by silicon chromatography using petroleum ether/dichloromethane (4:1 v/v) as eluent to give the product as a yellow solid (1.39 g, 82%). ^{1}H NMR (400 MHz, $CDCl_3$), δ (ppm): 7.88 (s, 1H), 7.86 (s, 1H), 7.39-7.42 (m, 2H), 7.31-7.32 (m, 2H), 7.08-7.12 (m, 2H), 4.21-4.28 (m, 4H), 1.15 (q, J_1 = 7.2 Hz, J_2 = 14.8 Hz, 6H). ^{13}C NMR (100 MHz, $CDCl_3$), δ (ppm): 167.55, 167.47,141.39, 141.34, 140.59, 140.29, 134.14, 133.90, 133.78, 133.13, 132.07, 131.92, 130.80, 127.39, 127.05, 126.61, 126.37, 120. 73, 120.56, 61.82, 61.74, 13.88, 13.79. HRMS (ESI) m/z: $[M + H]^+$ calcd. for $C_{24}H_{19}O_4S_4^+$, 499.01607, found 499.01617.

Synthesis of ***compound 4:*** To a stirring solution of compound **3** (500 mg, 1 mmol) in dry THF under argon condition was added (4-hexylphenyl)magnesium bromide which was prepared from 1-bromo-4-hexylbenzene (3.62 g, 15 mmol) and magnesium (396 mg, 16.5 mmol) in THF (10 ml). Then the mixed solution was heated to reflux for 16h. After cooling to room temperature, the solution was poured into water and extracted with ethyl acetate, then washed with saturated salt water several times and dried with anhydrous Na_2SO_4. After removal of the solvent under reduced pressure, the crude product was obtained and then used in the next step without further purification. The crude product was dissolved in chloroform/glacial acetic acid (5:1 v/v), and 1 ml concentrated sulfuric acid in 5 ml glacial acetic acid was dropwise added into the solution, then the mixture was refluxed for 30 min. After cooling to room temperature, the mixture was extracted with dichloromethane and washed with water. The collected organic layer was dried over anhydrous Na_2SO_4 and concentrated. The residue was purified by column chromatography on silica gel using a mixture solvent as eluent (petroleum ether/dichloromethane, v/v = 15/1) to give a yellow solid (357 mg, 35%). ^{1}H NMR (400 MHz, $CDCl_3$), δ (ppm): 7.52 (s, 1H), 7.46 (s, 1H), 7.28 (d, *J* = 5.2 Hz, 1H), 7.25 (d, *J* = 4.8 Hz, 1H), 7.18-7.21 (m, 9 H), 7.07-7.09 (m, 8H), 7.00 (d, *J* = 4.8 Hz, 1H), 2.53-2.59 (m, 8H), 1.56-1.61 (m, 8H), 1.27-1.36 (m, 24H), 0.85-0.89 (m, 12H). ^{13}C NMR (100 MHz, $CDCl_3$), δ (ppm): 155.98, 153.64, 153.09, 147.10, 141.94, 141.78, 141.43, 141.17, 141.10, 140.07, 136.01, 135.51, 135.47, 132.42, 131.64, 128.39, 128.29, 128.04, 127.87, 127.60, 125.37, 123.11, 120.63,

117.05, 63.00, 62.66, 35.56, 31.71, 31.68, 31.34, 31.28, 29.69, 29.15, 22.59, 22.57, 14.10, 14.09. HRMS (ESI) m/z: $[M + H]^+$ calcd. for $C_{68}H_{75}S_4^+$, 1019.47462, found 1019.47432.

Synthesis of ***compound 5:*** To a dry 100 mL two-necked round bottom flask, 10 ml anhydrous *N*, *N*-dimethylformamide (DMF) was added, and the solution was cooled to 0°C and stirred when 2 ml phosphorous oxychloride ($POCl_3$) was added by syringe under argon protection. The mixture kept at 0°C for one hour, and then compound **4** (330 mg, 0.32 mmol) in dry 1, 2-dichloroethane (20 ml) was added. Then, the mixture solution was allowed to reflux for 16h. After cooling to room temperature, 100 ml water was added to quench the reaction. The mixture was extracted with dichloromethane (DCM), then washed with water and dried with anhydrous Na_2SO_4. After removal of the solvent under reduced pressure, the residue was purified by column chromatography on silica gel using a mixture solvent as eluent (petroleum ether/dichloromethane, v/v = 1/1) to give a yellow solid (300 mg, 86%). ^{1}H NMR (400 MHz, $CDCl_3$), δ (ppm): 9.92 (s, 1H), 9.82 (s, 1H), 7.87 (s, 1H), 7.66 (s, 1H), 7.64 (s, 1H), 7.53 (s, 1H), 7.17 (d, *J* = 7.6 Hz, 8H), 7.11 (d, J = 7.6 Hz, 8H), 2.54-2.59 (m, 8H), 1.55-1.61 (m, 8H), 1.27-1.31 (m, 24H), 0.84-0.89 (m, 12H). ^{13}C NMR (100 MHz, $CDCl_3$), δ (ppm): 182.87, 182.71, 156.47, 155.17, 154.14, 150.80, 148.15, 145.85, 145.29, 143.32, 142.35, 142.13, 141.29, 140.72, 140.44, 139.11, 138.58, 137.33, 134.72, 133.05, 132.10, 130.09, 128.66, 128.60, 127.85, 127.67, 118.73, 117.75, 63.15, 62.92, 35.53, 31.68, 31.66, 31.32, 31.25, 29.11, 29.10, 22.57, 22.56,

14.09, 14.07. HRMS (ESI) m/z: $[M + H]^+$ calcd. for $C_{70}H_{75}O_2S_4^+$, 1075.46444, found 1075.46545.

*Synthesis of **MeIC1:*** To a 100 ml round bottom flask, compound **5** (150 mg, 0.14 mmol), CPTCN (119 mg, 0.56 mmol), chloroform (30 ml) were added under argon protection and stirred for a while when pyridine (1 ml) was added. The mixture was kept stirring at 70°C for 12h. After removal of chloroform of reaction mixture under reduced pressure, 100 ml methanol was added and the precipitate was collected by filtration. The residue was purified by column chromatography on silica gel using a mixture solvent as eluent (petroleum ether/dichloromethane, v/v = 2/3) to give a brownish red solid (175 mg, 85%).^{1}H NMR (400 MHz, $CDCl_3$), δ (ppm): 8.79 (s, 1H), 8.78 (s, 1H), 8.08 (s, 1H), 7.96 (s, 1H), 7.86 (s, 1H), 7.77 (s, 1H), 7.62 (s, 1H), 7.58 (s, 1H), 7.12-7.19 (m, 16H), 2.77 (s, 3H), 2.75 (s, 3H), 2.56-2.61 (m, 8H), 1.58-1.63 (m, 8H), 1.28-1.35 (m, 24H), 0.84-0.90 (m, 12H); ^{13}C NMR (100 MHz, $CDCl_3$), δ (ppm): 182.71, 182.61, 159.88, 157.50, 156.48, 155.98, 155.56, 154.89, 148.92, 147.89, 145.86, 145.05, 144.76, 142.87, 142.65, 142.58, 142.34, 142.13, 142.02, 140.80, 140.47, 139.40, 139.31, 138.89, 138.52, 138.26, 137.04, 136.86, 135.37, 133.83, 129.26, 128.87, 128.77, 128.67, 127.84, 127.81, 125.16, 119.64, 118.22, 115.12, 114.93, 114.59, 114.48, 67.29, 66.70, 63.22, 62.98, 35.61, 31.75, 31.73, 29.15, 29.14, 22.70, 22.64, 22.62, 14.17, 14.15, 13.55, 13.54. HRMS (ESI) m/z: $[M + H]^+$ calcd. for $C_{92}H_{83}N_4O_2S_6^+$, 1466.47620, found 1466.47573.

Measurements

^{1}H NMR and ^{13}C NMR spectra were recorded on a Bruker Advanced II (400 MHz) spectrometer using *d*-chloroform as solvent. The high resolution mass spectra (HRMS) were performed on Thermo Scientific LTQ Orbitrap Xl using ESI. UV-vis spectra were measured using a Shimadzu UV-2500 recording spectrophotometer. Cyclic voltammetry (CV) measurements of targeted SMAs thin films were conducted on a CHI voltammetric analyzer in acetonitrile solution with 0.1 M tetrabutylammonium hexafluorophosphate (*n*-Bu_4NPF_6) as supporting electrolyte at room temperature by using a scan rate of 100 mV s^{-1} and conventional three-electrode. Atomic force microscopy (AFM) images were obtained by using a NanoMan VS microscope in the tapping-model. Transmission electron microscopy (TEM) images of the active layers were obtained by using a JEOL JEM-1400 transmission electron microscope operated at 80 kV.

Devices fabrication and characterization

The conventional photovoltaic devices were fabricated with a structure of ITO/ PEDOT:PSS/PBDB-T:acceptor/PDIN/Al. First, the patterned ITO-coated glass with a sheet resistance of 15 Ω sq^{-1} was scrubbed by detergent and then cleaned inside an ultrasonic bath by using deionized water, acetone, and isopropyl alcohol sequentially. The ITO substrates was fast dried by using high pure nitrogen gas and then treated by oxygen plasma for 1 min to improve its work function and clearance. Then, PEDOT:PSS (Heraeus Clevios P VP A 4083) layer was spin-coated onto ITO

substrate with a thickness of about 40 nm and dried at 150°C for 10 minutes in air, and the PEDOT:PSS coated ITO substrates were fast transferred to a N_2 filled glove-box for further processing. The blend solution in chlorobenzene (CB) with a total concentration of 20 mg/ml (PBDB-T:acceptor (wt/wt:1:1)) and 0.5% DIO addition was drop-cast at the PEDOT:PSS layer at 2500 rpm for 1 min and controlled the active layer thickness of ~100 nm measured by Ambios Technology XP-2 stylus Profiler. After spin-coated, the active layer was annealed at 120°C for 8 minutes. Next, the methanol solution of PDIN of 1.0 mg/ml was deposited atop the active layer at 3000 rpm for 30 s to afford a PDIN cathode buffer layer with thickness of ca. 10 nm. Subsequently, the active layer coated substrates were quickly transferred to a glove-box integrated thermal evaporator for Al deposition. Al (100 nm) layers were evaporated onto the active layer through a shadow mask at a vacuum pressure of ≈ 5×10^{-5} Pa to form top electrode. The active area of cells is 3.8 mm^2, which is defined by the vertical overlap of ITO cathode and Al anode. The current-voltage (*J-V*) characteristic curves of all devices were measured by using a Keithley 2400 Source Meter in a high-purity nitrogen-filled glove box. AM 1.5G irradiation at 100 mW/cm^2 provided by a XES-40S2 (SAN-EI Electric Co., Ltd.) solar simulator (AAA grade, 70×70 mm^2 photobeam size), which was calibrated by standard silicon solar cells (purchased from Zolix INSTRUMENTS CO. LTD). The external quantum efficiency (EQE) spectra of all devices were measured in air conditions by a Zolix Solar Cell Scan 100.

SCLC measurements

The electron-only SCLC devices were a stack of ITO/ZnO/PBDB-T:acceptor/Al, and the hole-only devices were a stack of ITO/PEDOT:PSS/PBDB-T:acceptor/MoO_3/Ag. The electron-only and hole-only SCLC devices fabrication processing methods are same with those for solar cell. The charge carrier mobility was determined by fitting the dark current to the model of a single carrier SCLC according to the equation:

$$J = \frac{9\varepsilon_o\varepsilon_r\mu V^2}{8L^3}$$

where J is the current density, L is the film thickness of the active layer, μ is the charge carrier mobility, ε_r is the relative dielectric constant of the transport medium, and ε_0 is the permittivity of free space. $V = V_{app} - V_{bi}$, where V_{app} is the applied voltage, V_{bi} is the offset voltage. The carrier mobility can be calculated from the slope of the $J^{1/2} \sim V$ curves.

GIWAXS measurements

All tested samples were fabricated under the same condition of best-performance devices on the cleaned Si substrates. GIWAXS measurement was performed at beamline 7.3.3 at the Advanced Light Source of Lawrence Berkeley National Lab (LBNL). The 10 K eV X-ray beam was incident at a grazing angle of 0.12° – 0.16° to obtain optimal signal-to-background ratio. The scattered X-ray signals were detected by using a Dectris Pilatus 2M photon counting detector. The whole experiments were carried out in helium atmosphere.

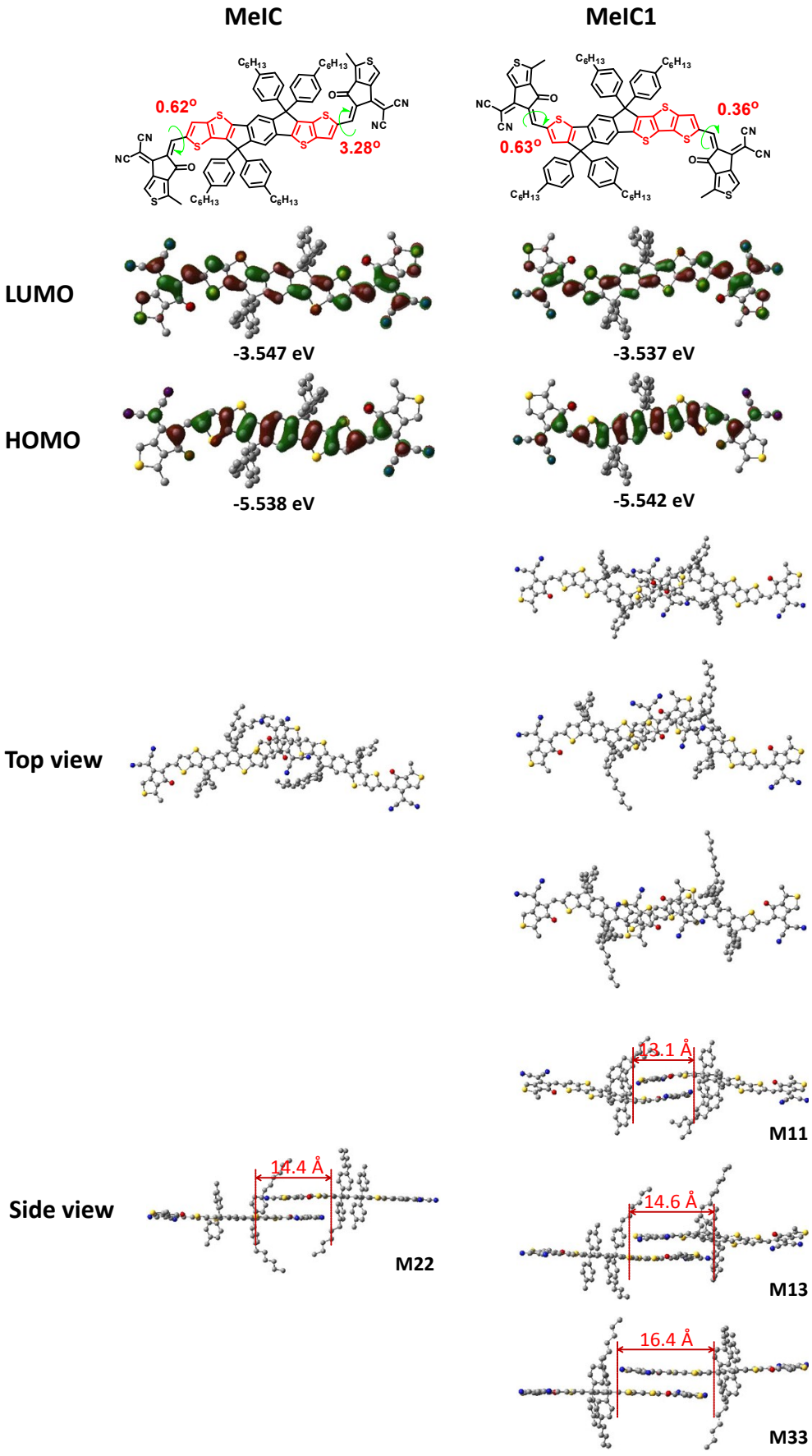

Fig. S1 Theoretical simulation results.

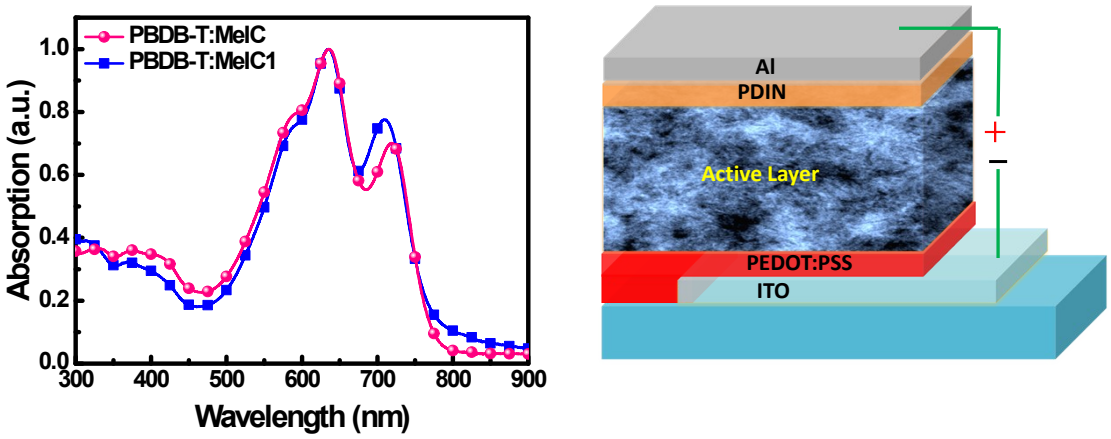

Fig. S2 The absorption spectra of active layers (left) and the device structure.

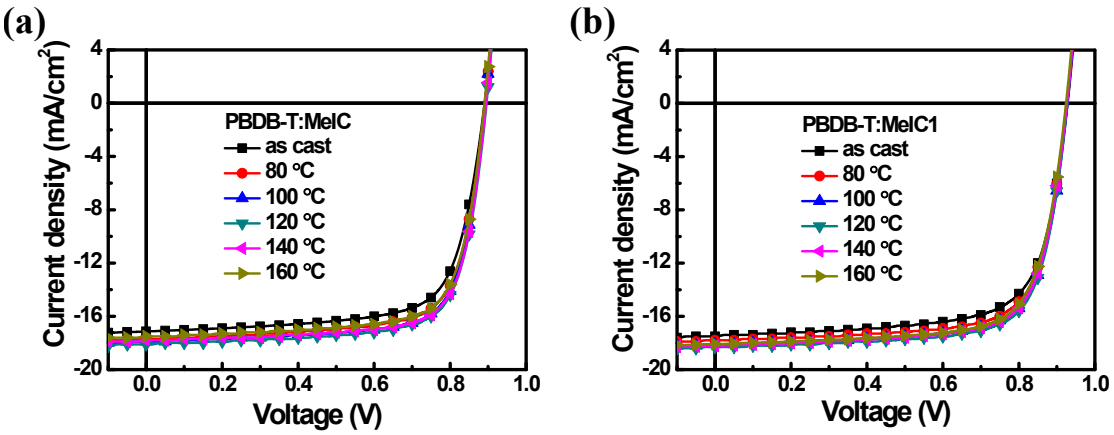

Fig. S3 The *J-V* curves of PBDB-T:MeIC (wt/wt, 1:1; 0.5% DIO) and PBDB-T:MeIC1 (wt/wt, 1:1; 0.5% DIO) under different annealed temperatures.

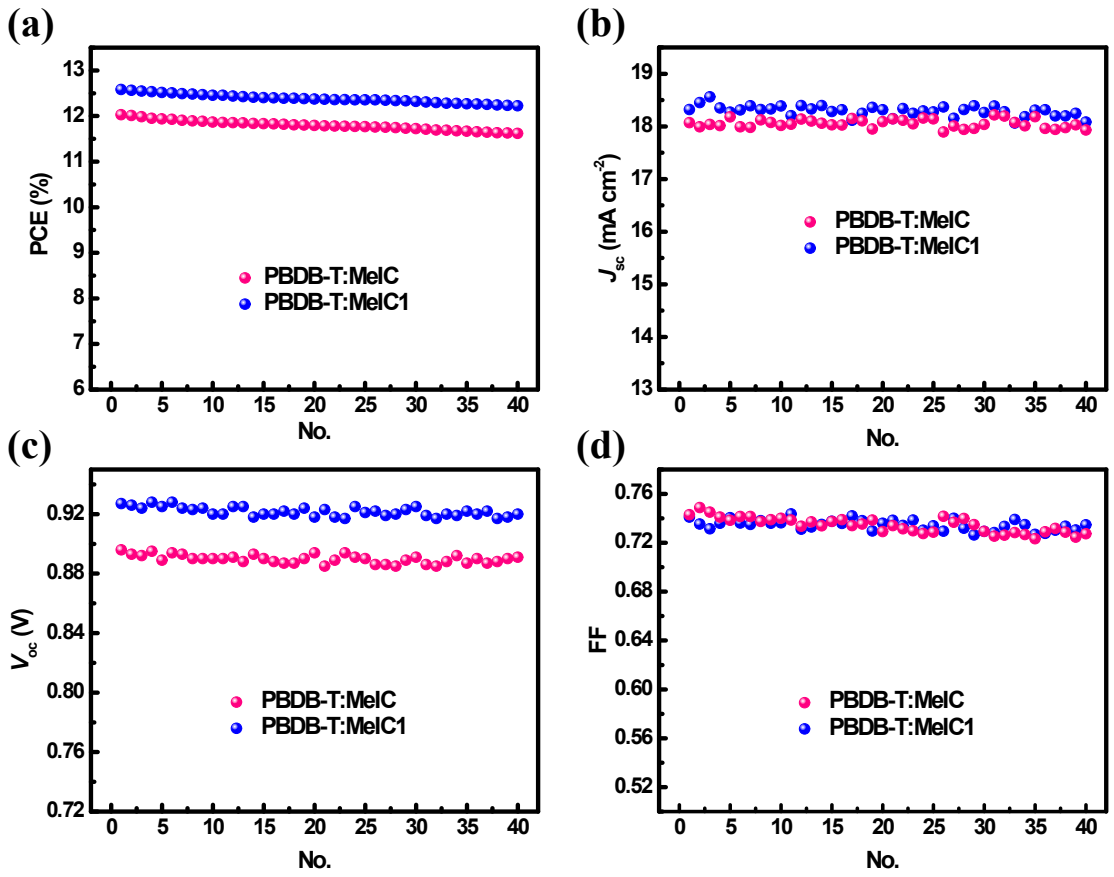

Fig. S4 The detailed photovoltaic parameters of typical 40 samples.

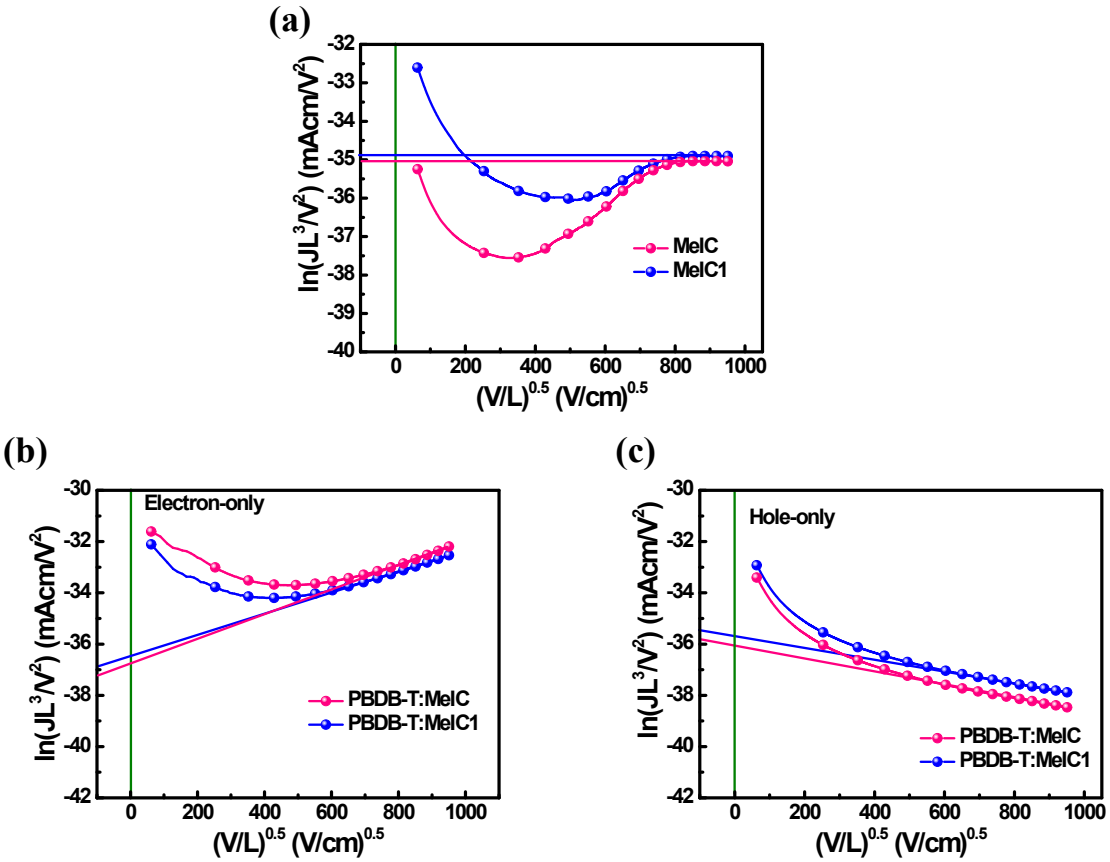

Fig. S5 a) The electron mobility of MeIC and MeIC1 neat films. b) The electron mobility of PBDB-T:MeIC and PBDB-T:MeIC1 blend films. c) The hole mobility of PBDB-T:MeIC and PBDB-T:MeIC1 blend films.

Table S1 The theoretical calculation parameters of dimer molecules for MeIC and MeIC1.

	stacking form	overlap length (Å)	intermolecular bonding energy (eV)	electron transfer integral (cm^{-1})	electron density overlap integral
MeIC	M22	14.4	-1.75	440	0.70
	M11	13.1	-2.36	352	1.05
MeIC1	M13	14.6	-1.99	466	0.82
	M33	16.4	-2.05	538	0.93

Table S2 The photovoltaic parameters of PBDB-T:MeIC (wt/wt, 1:1; 0.5% DIO) and PBDB-T:MeIC1 (wt/wt, 1:1; 0.5% DIO) under different annealed temperatures.

Acceptor	Annealed temperature (°C)	V_{oc} (V)	J_{sc} (mA cm^{-2})	FF	PCE (%)
MeIC	As cast	0.890	17.13	0.718	10.95
	80	0.891	17.69	0.733	11.56
	100	0.893	17.90	0.741	11.86
	120	0.896	18.07	0.743	12.03
	140	0.894	17.83	0.747	11.91
	160	0.890	17.53	0.739	11.53
MeIC1	As cast	0.927	17.47	0.715	11.57
	80	0.928	17.80	0.729	12.05
	100	0.928	18.12	0.735	12.36
	120	0.927	18.32	0.741	12.58
	140	0.926	18.22	0.734	12.40
	160	0.924	18.08	0.732	12.24

Table S3 Key photovoltaic parameters calculated from the J_{ph}-V_{eff} curves of optimal devices based on PBDB-T:MeIC and PBDB-T:MeIC1.

Active layer	J_{sat}[a] (mA cm^{-2})	J_{ph}^{*}[b] (mA cm^{-2})	$J_{ph}^{\&}$[c] (mA cm^{-2})	J_{ph}^{*}/J_{sat} (%)	$J_{ph}^{\&}/J_{sat}$ (%)
PBDB-T:MeIC	18.81	18.07	15.95	96.06	84.79
PBDB-T:MeIC1	18.91	18.32	15.97	96.88	84.45

[a]The J_{ph} under condition of V_{eff} = 2.2 V. [b]The J_{ph} under short circuit condition. [c]The J_{ph} under maximum power output condition.

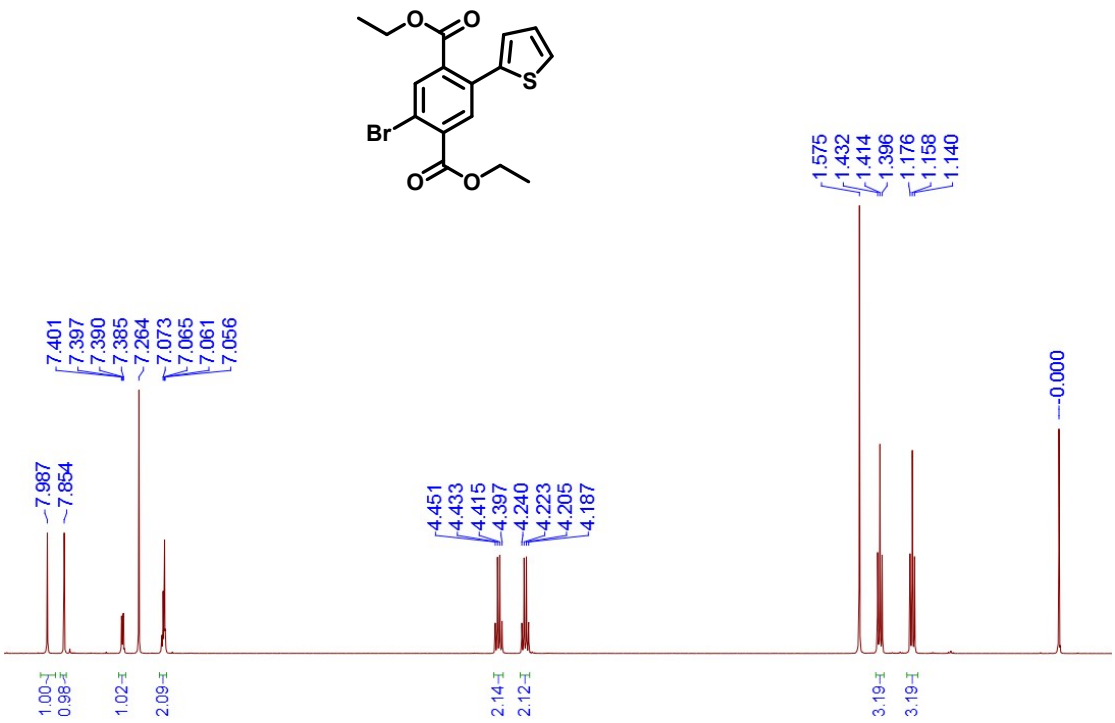

Fig. S6 The ^{1}H NMR spectrum of **compound 2** in $CDCl_3$.

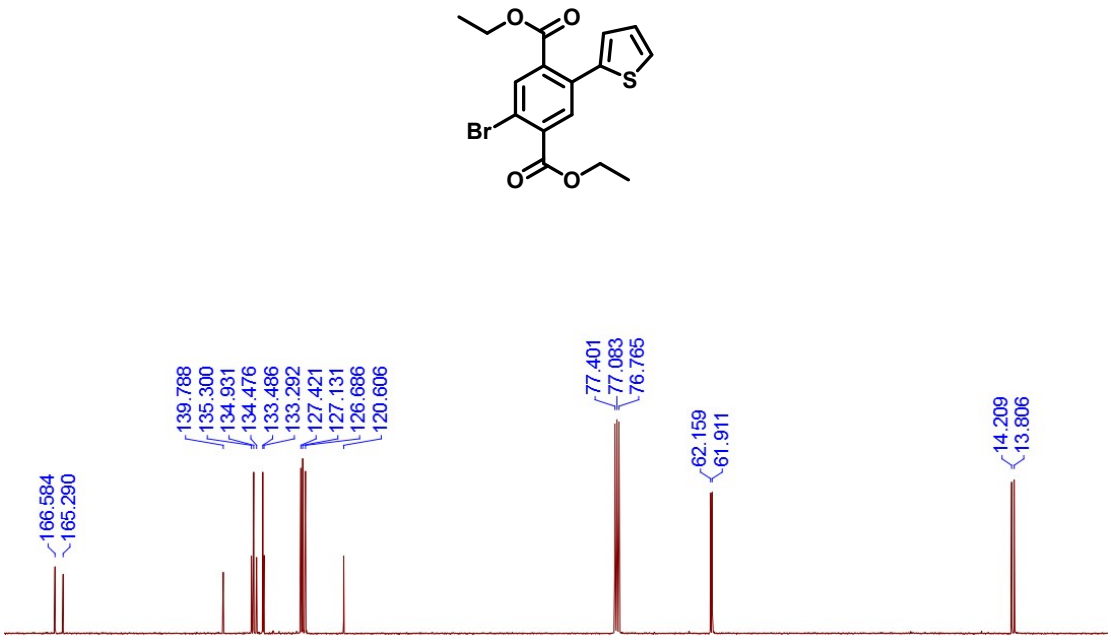

Fig. S7 The ^{13}C NMR spectrum of **compound 2** in $CDCl_3$.

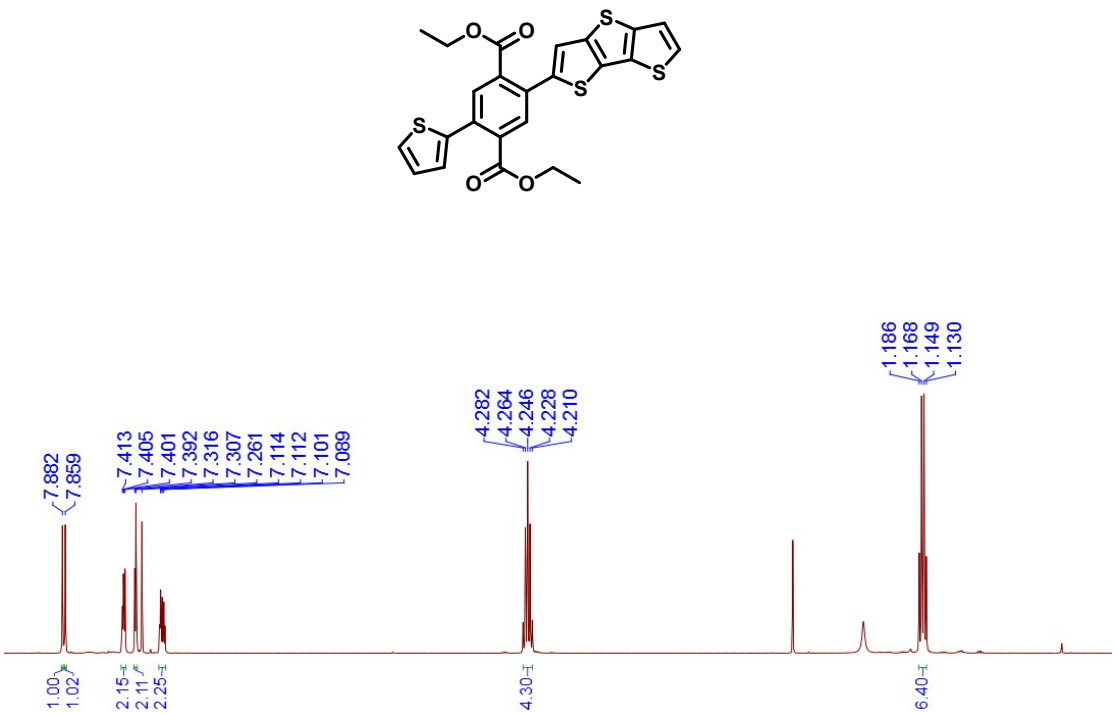

Fig. S8 The ^{1}H NMR spectrum of **compound 3** in $CDCl_3$.

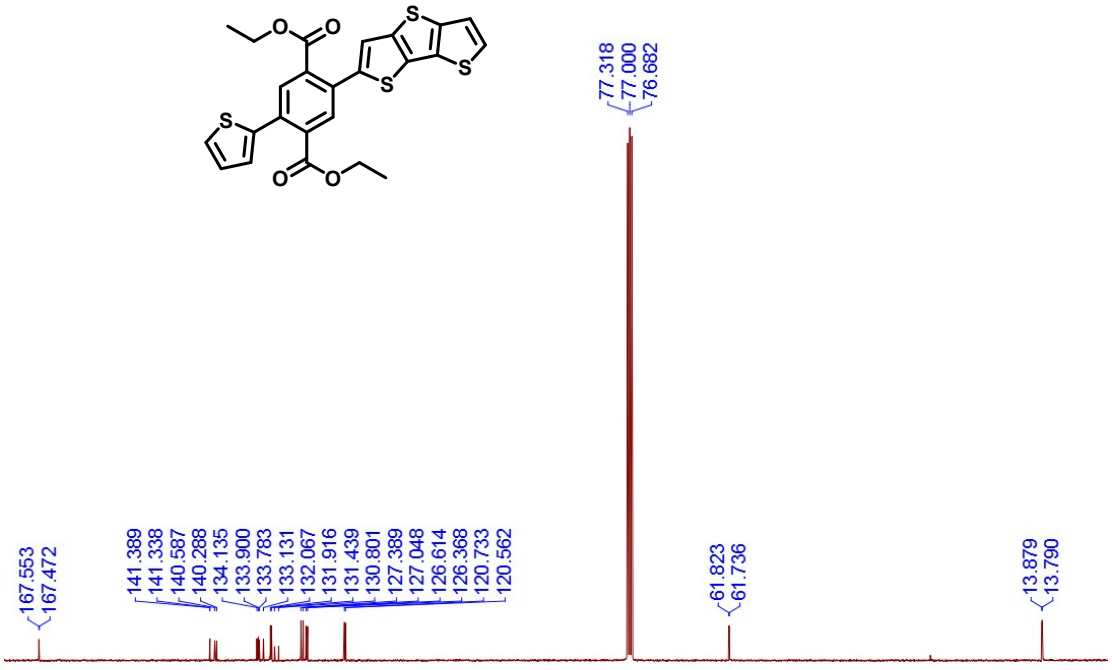

Fig. S9 The ^{13}C NMR spectrum of **compound 3** in $CDCl_3$.

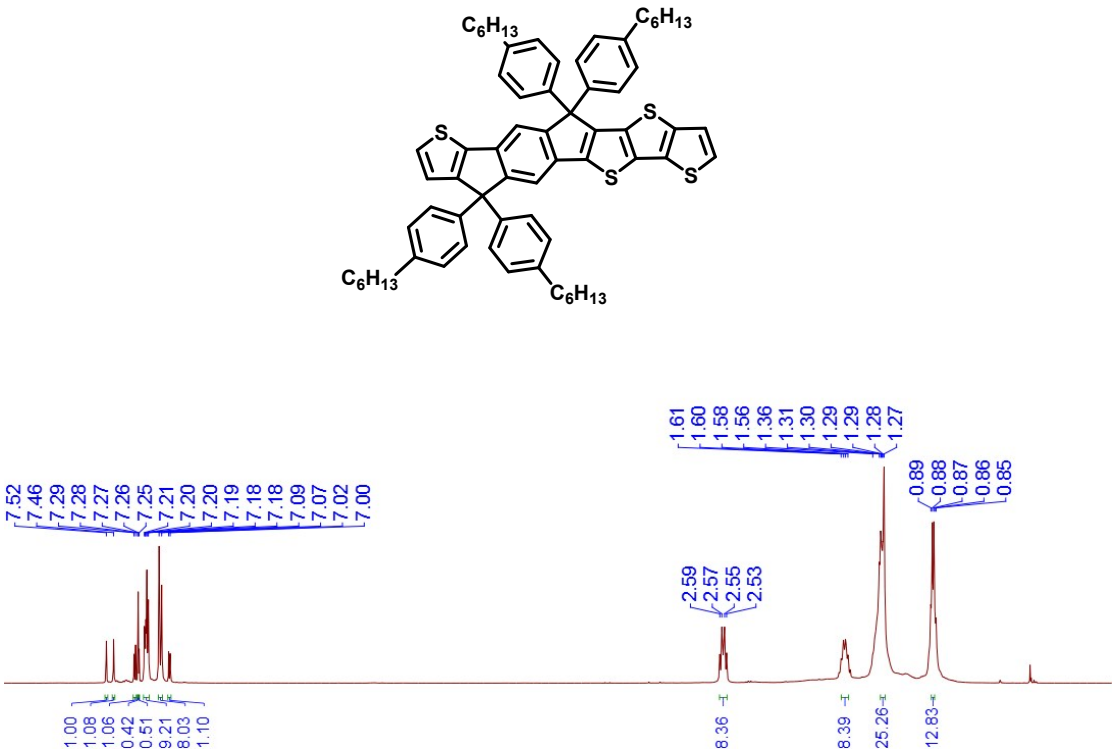

Fig. S10 The ^{1}H NMR spectrum of **compound 4** in $CDCl_3$.

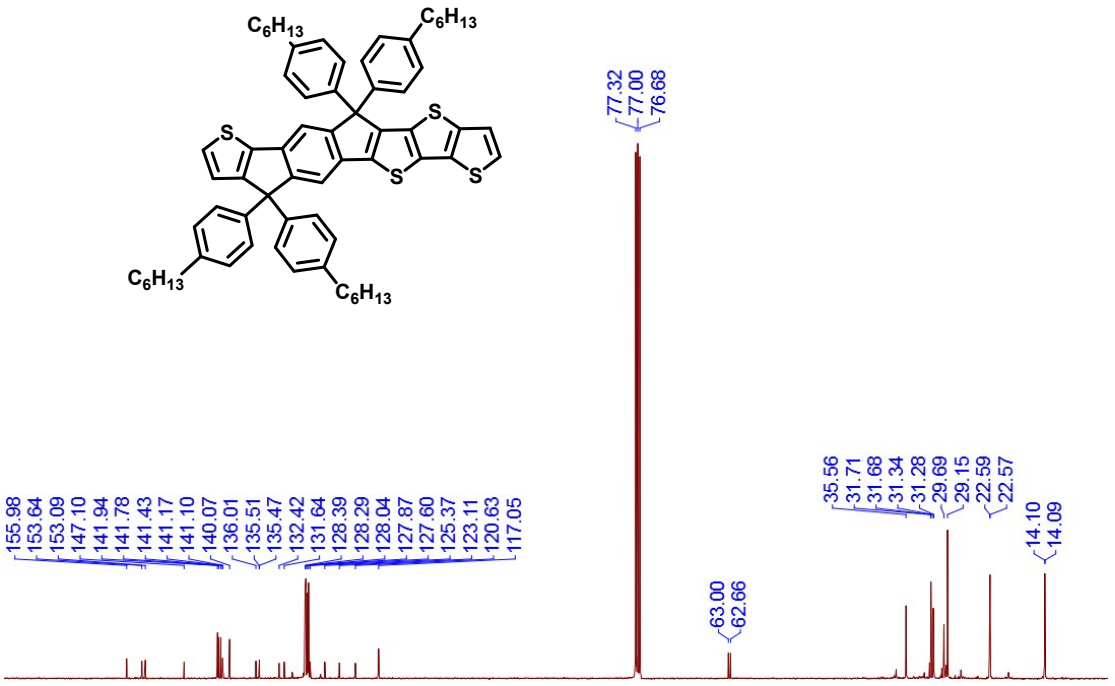

Fig. S11 The ^{13}C NMR spectrum of **compound 4** in $CDCl_3$.

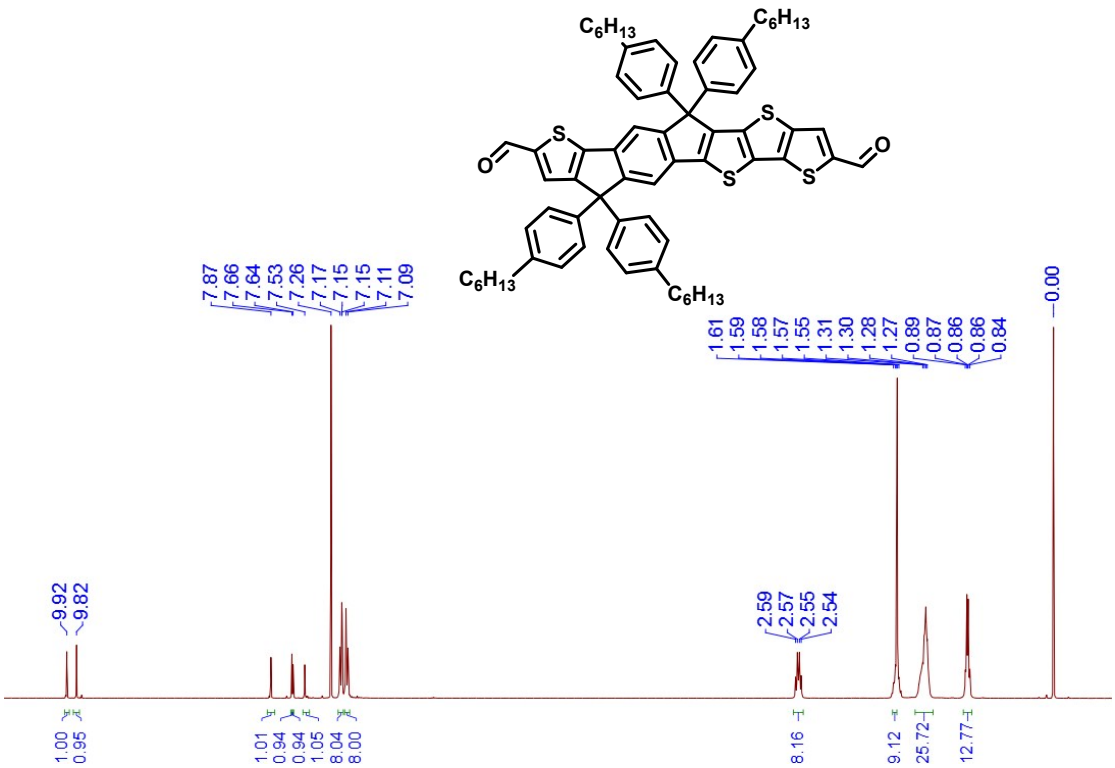

Fig. S12 The ^{1}H NMR spectrum of **compound 5** in $CDCl_3$.

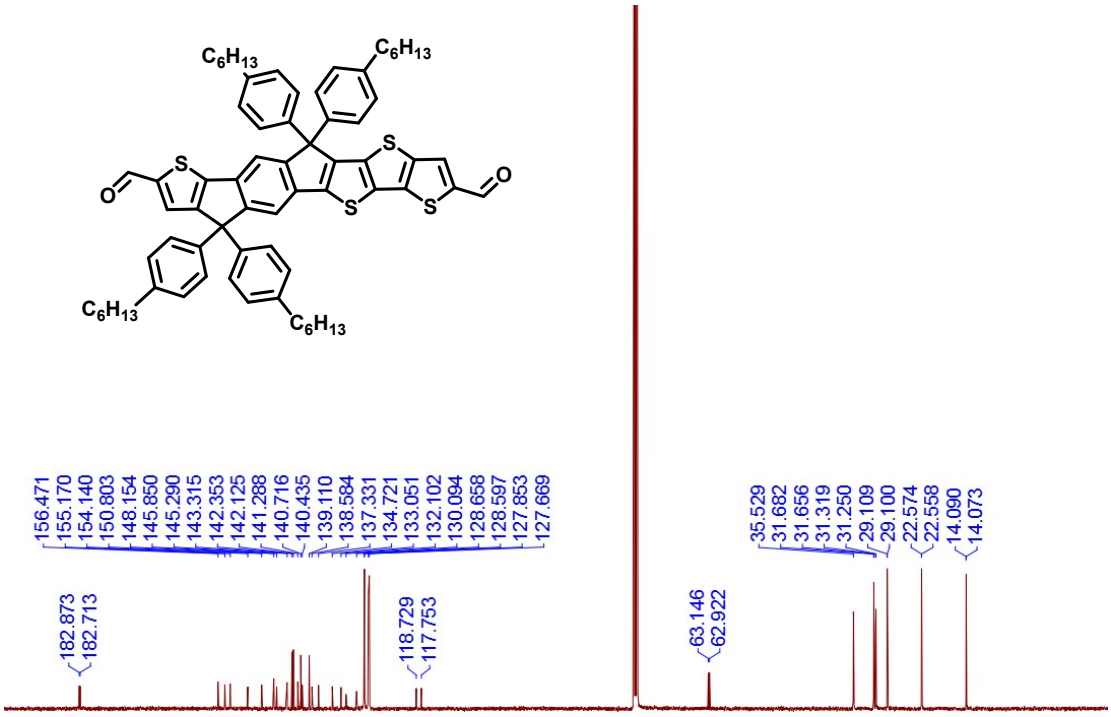

Fig. S13 The ^{13}C NMR spectrum of **compound 5** in $CDCl_3$.

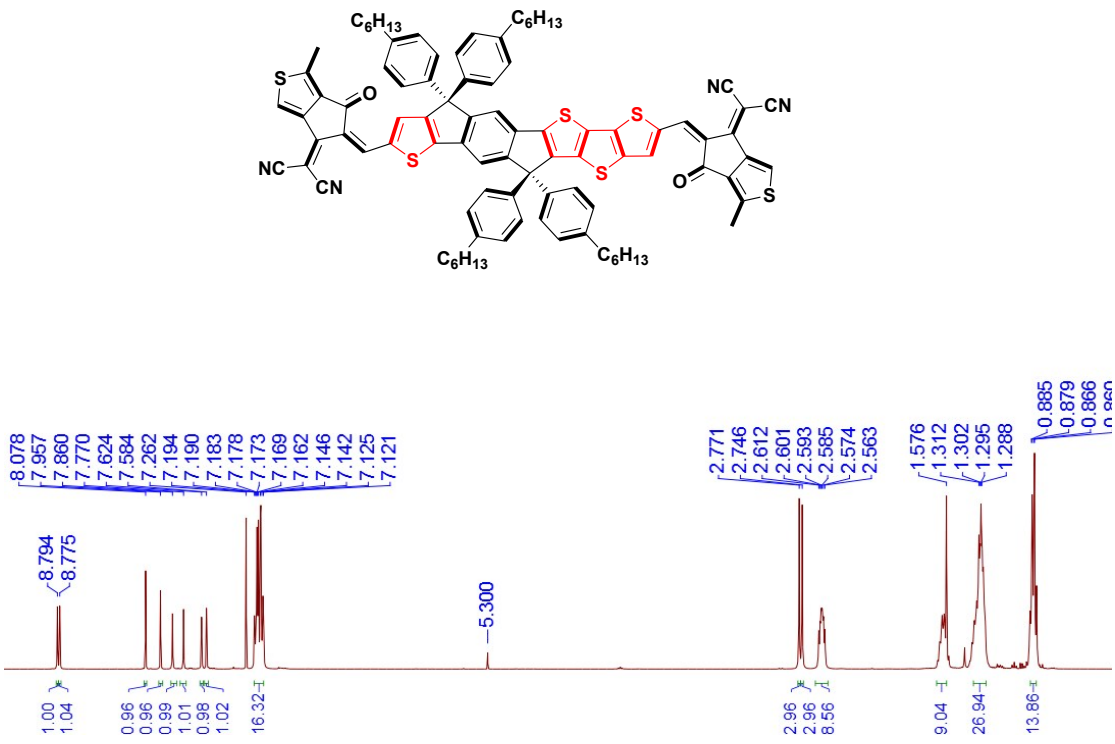

Fig. S14 The ^{1}H NMR spectrum of **MeIC1**in $CDCl_3$.

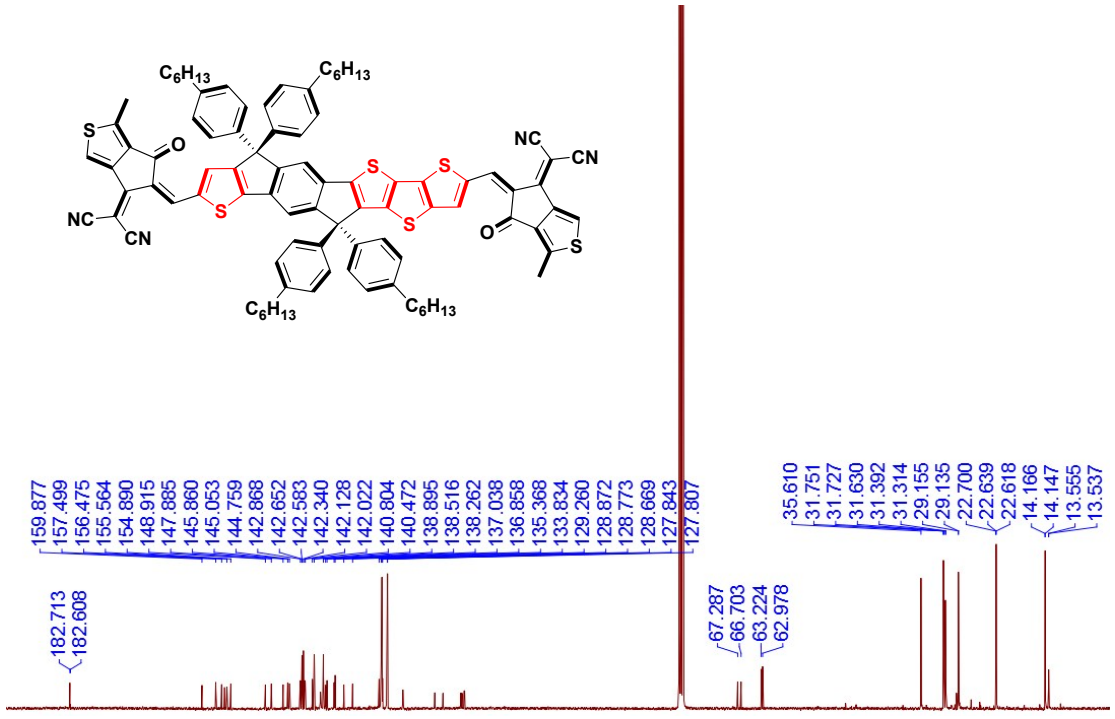

Fig. S15 The ^{13}C NMR spectrum of **MeIC1** in $CDCl_3$.